Calculation of Plasma Properties in Ion Sources

John R. Brophy* and Paul J. Wilbur†
Colorado State University, Fort Collins, Colorado

Simple algebraic equations are developed that can be used to calculate the average primary electron density, the average primary-to-total electron density ratio, and the average Maxwellian electron temperature in the discharge chamber of a cusped magnetic field ion source. These properties may be calculated as functions of the propellant gas flow rate and the propellant utilization efficiency. Each of the plasma properties calculated using the model agree well with the corresponding experimental data for both argon and xenon gases over a wide range of propellant flow rates and utilization efficiences.

Nomenclature

A_g = area of grids through which the ion beam is extracted, m^2
E = electron energy, eV
e = electronic charge, 1.6×10^{-19} C
f_B = extracted ion fraction
J_B = ion beam current, A
J_E = cathode emission current, A
J'_{ex} = total production rate of excited neutral atoms by primary electrons, expressed as a current, A
J_{L_i} = primary electron current to the anode, A
J_p = total ion production rate, expressed as a current, A
J'_p = ion production rate by primary electrons, expressed as a current, A
$J_{P,M}$ = ion production rate by Maxwellian electrons, expressed as a current, A
l_e = primary electron containment length, m
m_e = electron mass, kg
$\dot{m}$ = thruster propellant flow rate, equivalent A
n_i = total ion density, m^{-3}
n_M = Maxwellian electron density, m^{-3}
n_p = primary electron density, m^{-3}
n_0 = neutral atom density, m^{-3}
$\dot{n}_0$ = neutral atom loss rate, equivalent A
Q_0^+ = Maxwellian electron rate factor for ionization of neutral atoms, m^3/s
T_A = Maxwellian electron temperature at anode surface, eV
T_M = Maxwellian electron temperature in bulk plasma, eV
U_{ex} = lumped excitation energy, eV
U_+ = ionization energy, eV
U_j = excitation energy of jth excited state, eV
U_l = lowest excitation energy, eV
V_A = anode sheath voltage, V
V_C = plasma potential from which electrons emitted by the cathode are accelerated to become primary electrons, V
V_D = discharge voltage, V
v_b = Bohm velocity, m/s
v_e = electron velocity, m/s
v_p = primary electron velocity, m/s
v_0 = neutral atom velocity, m/s
$\mathcal{V}$ = volume of ion production region, m^3
ϵ_M = average energy of Maxwellian electrons leaving the plasma at the anode, eV
ϵ_p = average plasma ion energy cost, eV/plasma ion
ϵ_p^* = baseline plasma ion energy cost, eV/plasma ion
ϵ_0 = average plasma ion energy cost considering ionization and excitation processes only, eV
η_u = propellant utilization efficiency
σ_j = excitation collision cross section of the jth state, m^2
σ'_j = excitation collision cross section of the jth state at the primary electron energy, m^2
σ'_0 = total inelastic collision cross section at the primary electron energy, m^2
σ_+ = ionization collision cross section, m^2
σ'_+ = ionization collision cross section at the primary electron energy, m^2
ϕ_a = transparency of the accelerator grid to neutral atoms
ϕ_i = transparency of the screen grid to ions
ϕ_s = transparency of the screen grid to neutral atoms
ϕ_0 = effective transparency of the grid system to neutral atoms

Introduction

In the design of broad-beam, electron bombardment ion sources for both space propulsion and ground-based applications it is generally desirable to predict discharge chamber plasma properties so such quantities as doubly charged ion density levels and discharge chamber sputtering rates can be computed. A recently proposed model[1] of discharge chamber operation, which relates the energy cost of producing a beam ion to the propellant utilization efficiency, has been extended to facilitate the calculation of these plasma properties. In particular, simple algebraic relationships are developed for the calculation of the following average discharge chamber plasma properties: primary electron density, primary-to-Maxwellian electron density ratio, and Maxwellian electron temperature.

Theoretical Development

Assumptions and Limitations

This theoretical development is applicable to cusped magnetic field discharge chambers that produce a steady-state, low-pressure, partially ionized, optically thin plasma. Neutral densities for these chambers are typically in the range of 10^{18}-10^{19} m^{-3} and plasma densities of 10^{16}-10^{17} m^{-3}. The Maxwellian electron temperatures and primary electron energies are 1-10 and 20-50 eV, respectively. Electron energy losses due to elastic collisions with ions or neutral atoms are neglected in the development, as are losses resulting from inelastic electron-ion collisions. The elastic collision losses can be neglected because the average energy loss per encounter is proportional to the ratio of masses, which is small ($\sim 10^{-5}$). The inelastic electron-ion collisions may be neglected because of the low ion density relative to the neutral density. The

Received Feb. 15, 1985; revision submitted Feb. 11, 1986.

*Research Assistant, Department of Mechanical Engineering (presently with the Jet Propulsion Laboratory, Pasadena, CA). Member AIAA.
†Professor, Department of Mechanical Engineering. Member AIAA.

effect of metastable atomic states on ion production is also neglected.

Further, primary electron thermalization resulting from collisions with the background Maxwellian electrons is neglected. Primary electron behavior is assumed to be limited to either inelastic collisions with neutral atoms or direct loss to anode potential surfaces. A primary electron is considered to join the Maxwellian electron population after having one inelastic collision.

Electrons are assumed to be constrained by the plasma sheaths, so they are able to leave the plasma only at the anode potential surfaces. Ions and photons (emitted by the de-excitation of excited propellant atoms) are assumed to be lost across all plasma boundaries. The assumption of a low-pressure discharge implies that ion-electron recombination should be well controlled; consequently, volume ion recombination is neglected.

The neutral atom density is assumed to be uniform throughout the discharge chamber and free molecular flow is assumed to apply to the neutral atom flux through the accelerator grid system.

Primary Electron Density

This analysis is based on the recognition that all of the energy supplied to the discharge chamber plasma is supplied by the primary electrons. Thus, correctly accounting for the behavior of the primary electrons is essential in determining the average plasma properties. It is assumed that a primary electron can do only one of two things. It can either have an inelastic collision with a neutral propellant atom or it can be lost directly to the anode. For the case where the primary electron has an inelastic collision with a neutral atom, it will produce either an ion or an excited neutral state. After such an inelastic collision, the energy of the primary electron is degraded and it is assumed that it is subsequently thermalized into the Maxwellian electron population. The rate at which primary electrons have inelastic collisions with neutral atoms is given by the difference between the rate at which they are supplied by the cathode J_E and the rate at which they are lost directly to the anode J_L, i.e.,

$$J_E - J_L = J_p' + J_{ex}' \tag{1}$$

where J_p' is the ion current produced by primary electrons and J_{ex}' the primary electron-induced production rate of excited neutral states expressed as a current. The ion current produced by primary electrons is given by

$$J_p' = n_0 n_p e \sigma_+' V v_p \tag{2}$$

and the rate of production of excited state atoms induced by primaries is given by

$$J_{ex}' = n_0 n_p e v_p V \sum_j \sigma_j' \tag{3}$$

Combining Eqs. (2) and (3), the fraction of the primary electronneutral atom inelastic collisions that produce ions is given by

$$\frac{J_p'}{J_p' + J_{ex}'} = \frac{\sigma_+'}{\sigma_0'} \tag{4}$$

where, $\sigma_0' = \sigma_+' + \Sigma_j \sigma_j'$. Multiplying Eq. (4) by the rate at which primary electron-neutral atom collisions occur [Eq. (1)] yields the rate at which ions are produced by primary electrons, i.e.,

$$J_p' = (J_E - J_L)\frac{\sigma_+'}{\sigma_0'} \tag{5}$$

The term in parentheses in Eq. (5) may be written as

$$J_E - J_L = J_E(1 - J_L/J_E) \tag{6}$$

The quantity J_L/J_E is the fraction of the input primary electron current lost directly to the anode and is given as[1]

$$J_L/J_E = e^{-\sigma_0' n_0 l_e} \tag{7}$$

where l_e, the primary electron containment length, represents the average distance a primary electron would travel in the discharge chamber before being collected by the anode if it had no inelastic collisions.

The average energy required to produce an ion in the discharge chamber plasma ϵ_p is defined by

$$\epsilon_p = J_E V_D / J_p \tag{8}$$

Solving Eq. (8) for J_E yields

$$J_E = J_p \epsilon_p / V_D \tag{9}$$

Combining Eqs. (5-7) and (9) yields an expression for the ratio of ion current produced by primaries to the total ion current produced,

$$\frac{J_p'}{J_p} = \frac{\epsilon_p \sigma_+'}{V_D \sigma_0'}\left(1 - e^{-\sigma_0' n_0 l_e}\right) \tag{10}$$

The average plasma ion energy cost ϵ_p, however, is given as[1]

$$\epsilon_p = \epsilon_p^*\left(1 - e^{-\sigma_0' n_0 l_e}\right)^{-1} \tag{11}$$

A simple method for the calculation of ϵ_p^* is developed in the Appendix of this paper.

Combining Eqs. (10) and (11) yields

$$\frac{J_p'}{J_p} = \frac{\epsilon_p^* \sigma_+'}{V_D \sigma_0'} \tag{12}$$

Since the ratio J_p'/J_p cannot be greater than one, Eq. (12) provides a theoretical limit for the maximum value of ϵ_p^*, i.e.,

$$(\epsilon_p^*)_{\max} = V_D \sigma_0'/\sigma_+' \tag{13}$$

The total ion current produced may be expressed in terms of the beam current J_B by using the definition[1] of the extracted ion fraction f_B

$$f_B = J_B/J_p \tag{14}$$

In addition, using the definition of the propellant utilization η_u, the beam current may be written as

$$J_B = \dot{m}\eta_u \tag{15}$$

Combining Eqs. (12), (14), and (15) yields

$$J_p' = \frac{\dot{m}\eta_u \epsilon_p^* \sigma_+'}{f_B V_D \sigma_0'} \tag{16}$$

Equating Eqs. (2) and (16) and solving for the primary electron density n_p yields

$$n_p = \frac{\epsilon_p^* \dot{m}\eta_u}{v_p V f_B V_D \sigma_0' e n_0} \tag{17}$$

The neutral atom density n_0 may be expressed in terms of the gas flow rate $\dot{m}$ and the propellant utilization efficiency η_u by equating the rate at which propellant enters and leaves the

discharge chamber, i.e.,

$$\dot{m} = J_B + \dot{n}_0 \tag{18}$$

The neutral flow rate from the discharge chamber may be calculated from the kinetic theory of gases as

$$\dot{n}_0 = \tfrac{1}{4} n_0 e v_0 A_g \phi_0 \tag{19}$$

Combining Eqs. (18) and (19) and using the definition of the propellant utilization yields

$$n_0 = \frac{4\dot{m}(1-\eta_u)}{e v_0 A_g \phi_0} \tag{20}$$

Finally, substituting this into Eq. (17) yields an expression for the average primary electron density as a function of the propellant utilization efficiency,

$$n_p = \left(\frac{\epsilon_p^* A_g \phi_0 v_0}{4 v_p \mathcal{V} f_B V_D \sigma_0'}\right) \frac{\eta_u}{1-\eta_u} \tag{21}$$

Remarkably, this expression does not depend on either the propellant flow rate or the primary electron containment length, both of which cancelled out in the analysis. The combination of parameters in the parentheses should be roughly a constant for a given discharge chamber configuration, propellant gas, and discharge voltage. Equation (21) indicates that the primary electron density is small at low propellant utilizations and increases dramatically as η_u approaches unity. At propellant utilizations close to one, the model breaks down because the ion density becomes comparable to the neutral atom density and electron-ion inelastic collisions can no longer be neglected.

Primary-to-Maxwellian Electron Density Ratio

Assuming quasi-neutrality, the average ion density n_i is equal to the average total electron density, i.e.,

$$n_i = n_p + n_M \tag{22}$$

where n_M is the Maxwellian electron density. In addition, the average ion density is related to the beam current by

$$J_B = 0.6 n_i e v_b A_g \phi_i \tag{23}$$

where v_b is the Bohm velocity.[2] Solving this equation for n_i and dividing the result into Eq. (21) yields the following expression for the average ratio of primary-to-total electron density:

$$\frac{n_p}{n_i} = \left[\frac{0.15 e \epsilon_p^* v_b A_g^2 \phi_0 \phi_i}{v_p V_D f_B \mathcal{V} \sigma_0'}\right] \frac{1}{\dot{m}(1-\eta_u)} \tag{24}$$

This equation indicates that the average primary-to-total electron density ratio should be a function of the neutral density parameter $\dot{m}(1-\eta_u)$. As was the case for Eq. (21), the combination of parameters in the square brackets of Eq. (24) should be roughly a constant for a given thruster design, propellant, and discharge voltage.

The primary-to-Maxwellian electron density ratio may be found by dividing Eq. (22) by n_p and solving for n_p/n_M,

$$\frac{n_p}{n_M} = \frac{1}{n_i/n_p - 1} \tag{25}$$

Thus, once the ratio n_p/n_i is calculated from Eq. (24) the primary-to-Maxwellian electron density ratio may be calculated from Eq. (25).

Maxwellian Electron Temperature

The total ion current produced J_p is the sum of the ion current produced by primary electrons J_p' and that produced by Maxwellian electrons $J_{P,M}$, i.e.,

$$J_p = J_p' + J_{P,M} \tag{26}$$

The ion current produced by primary electrons is given by Eq. (16) and that produced by Maxwellian electrons is given by

$$J_{P,M} = n_0 n_M e \mathcal{V} Q_0^+ \tag{27}$$

Combining Eqs. (14-16), (26), and (27) and solving for Q_0^+ yields

$$Q_0^+ = \frac{\dot{m}\eta_u}{f_B e \mathcal{V} n_0 n_M}\left(1 - \frac{\epsilon_p^* \sigma_+'}{V_D \sigma_0'}\right) \tag{28}$$

Using Eq. (20) for the neutral atom density allows Eq. (28) to be written as

$$Q_0^+ = \frac{v_0 A_g \phi_0}{4 \mathcal{V} f_B}\left(\frac{\eta_u}{1-\eta_u}\right)\left(\frac{1}{n_p}\right)\left(\frac{n_p}{n_M}\right)\left(1 - \frac{\epsilon_p^* \sigma_+'}{V_D \sigma_0'}\right) \tag{29}$$

Finally, combining Eqs. (17), (24), (25), and (29) yields

$$Q_0^+ = \frac{v_p \sigma_+' \left[\left(V_D \sigma_0'/\epsilon_p^* \sigma_+'\right) - 1\right]}{\alpha \dot{m}(1-\eta_u) - 1} \tag{30}$$

where

$$\alpha = \frac{v_p V_D \sigma_0' \mathcal{V}}{0.15 e \epsilon_p^* v_0 v_b A_g^2 \phi_0 \phi_i} \tag{31}$$

Equation (30) provides an expression for the Maxwellian electron ionization rate factor as a function of the neutral density parameter $\dot{m}(1-\eta_u)$. Once this rate factor has been calculated, it can be compared to a tabulation of rate factors vs electron temperature for the given propellant to determine the appropriate Maxwellian electron temperature. Equation (30) indicates that the average Maxwellian electron temperature should increase with decreasing values of the neutral density parameter.

Experimental Results and Discussion

Apparatus

For this investigation, the ion source shown schematically in Fig. 1 was designed and built. This source produces a 12 cm diam ion beam and provides the capability for measuring the distribution of ion currents to the beam, screen grid, and internal thruster surfaces (with the exception of the anode).

The magnetic field for the experimental ion source in Fig. 1 is established through the use of $1.9 \times 1.3 \times 0.5$ cm samarium cobalt permanent magnets. These permanent magnets are arranged end-to-end to form ring magnets of alternate polarity in the manner suggested by Fig. 1. The flux density at the surface of the magnets is 0.27 T and the magnets are attached to the steel discharge chamber housing by their own magnetic attraction. This arrangement allows the ion source magnetic field configuration to be altered quickly and easily by simply adding, removing, or changing the position of the magnets. Although many different configurations were tested, the results obtained were all similar; thus, only those obtained using the configuration shown in Fig. 1 will be presented. For this configuration, the upstream magnet ring is covered with a strip of 0.13 mm thick steel insulated from the magnets themselves by a strip of 0.25 mm thick flexible mica. This is done so that the surface of this strip can be maintained at the anode potential, while the rest of the thruster body is biased

negative of the cathode potential. The downstream magnet ring is uncovered.

The main discharge chamber cathode consists of seven 0.25 cm diam tungsten wires connected in parallel and supported by two support posts that are electrically isolated from the thruster body. Each cathode wire is approximately 2.8 cm long, so the total cathode length exposed to the plasma is about 19.6 cm. These seven short wires in parallel are used to minimize the voltage drop across the cathode. A voltage drop less than 3 V at the maximum heater current was achieved with this system. The small voltage drop across the cathode results in a primary electron energy distribution that more closely resembles the monoenergetic distribution produced by a hollow cathode. The cathode wires were heated using direct currents in the range of 6-8 A per wire. Tests were conducted using argon and xenon propellants. Discharge voltages were varied at 30-50 V for argon and 20-40 V for xenon. The discharge current was adjusted through the range of 0.5-5 A by controlling the heating current through the refractory cathode wires.

The source was equipped with two Langmuir probe assemblies. The first probe consisted of a 0.76 mm diam tantalum wire, 4.32 mm long, supported from a quartz tube insulator. This probe was positioned along the thruster centerline approximately half way between the cathode assembly and the screen grid as suggested in Fig. 1. The second probe was a square piece of steel, 1 cm on a side and 0.127 mm thick that was positioned on the surface of the upstream magnetic ring. This probe was insulated from the magnet ring with a piece of 0.13 mm thick flexible mica.

The ion accelerator system consisted of a set of dished small-hole accelerator grid (SHAG) optics with a cold-grid separation of 0.75 mm and screen and accelerator grid physical open area fractions of 0.68 and 0.30, respectively. All tests were conducted in a 1.2 m diam $\times$ 4.6 m long vacuum test facility. Indicated tank pressures ranged from $\sim 8 \times 10^{-6}$-3×10^{-5} Torr during testing.

Primary Electron Density

Equation (21) provides a simple expression for the primary electron density as a function of the propellant utilization. As mentioned earlier, the combination of parameters inside the parentheses in this equation may be taken to be roughly a constant for a given propellant, discharge voltage, and thruster configuration. The value of this constant, appropriate for argon propellant, a discharge voltage of 50 V, and the thruster configuration of Fig. 1, was calculated to be 1.0×10^{10} cm^{-3}. Thus, Eq. (21) becomes, in this case,

$$n_p = (1.0 \times 10^{10})\eta_u/(1-\eta_u), \text{ cm}^{-3} \qquad (32)$$

The value of ϵ_p^*, required for this calculation, was taken to be its value determined experimentally by the method described in Ref. 3. The value of ϵ_p^* could, however, have been calculated using the method described in the Appendix.

The volume of the ion production region $\mathcal{V}$, required by Eq. (21), was determined from a computer drawn magnetic field map of the discharge chamber. This map was created by measuring the magnetic flux density and direction at regularly spaced points in the discharge chamber. The ion production volume defined by this map was taken to be the volume in which the magnetic flux density was 0.005 T or less.

The extracted ion fraction f_B was taken to be its measured value obtained in tests with argon propellant, a discharge voltage of 50 V, and the thruster configuration of Fig. 1. The effective transparency of the grids to neutral atoms ϕ_0 was calculated from

$$\phi_0 = \frac{\phi_s \phi_a}{\phi_s + \phi_a} \qquad (33)$$

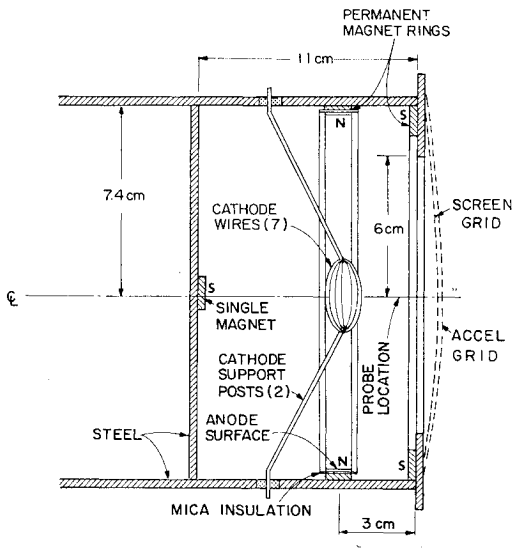

Fig. 1 Ring cusp ion source schematic.

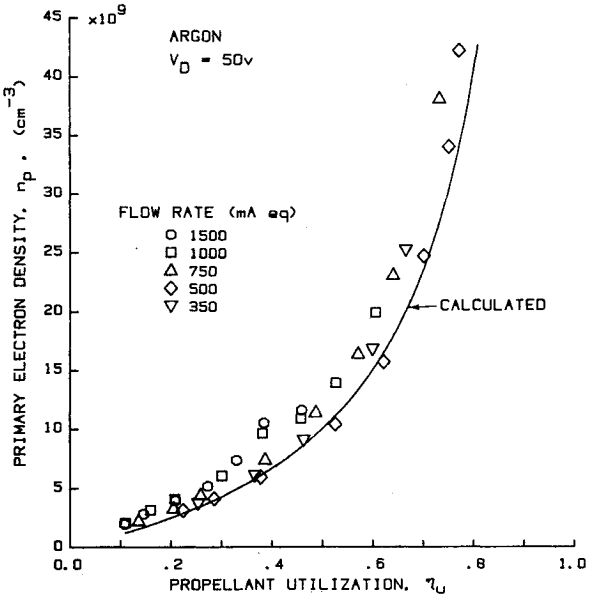

Fig. 2 Primary electron density variation for argon.

where ϕ_s and ϕ_a are the modified transparencies for the screen and accelerator grid, respectively. These modified transparencies may be calculated as the physical open area fraction of a grid times the appropriate Clausing factor.[4] Finally, the neutral atom velocity v_0 was calculated based on an assumed effective wall temperature of 400 K.

Comparison of the calculated values of the primary electron density from Eq. (32) with the measured values is given in Fig. 2. The measured primary electron densities were obtained using the Langmuir probe positioned along the centerline of the discharge chamber. Equation (32), however, yields essentially an average primary electron density. Further, since the centerline primary electron density is expected to be higher than the average value, the excellent agreement between the calculated and measured values in Fig. 2 is somewhat misleading. This figure clearly indicates, however, that Eq. (32) has the correct functional form and that the primary electron density is indeed relatively independent of the propellant flow rate as predicted by the model.

A similar comparison between calculated and measured primary electron densities is given in Fig. 3 for operation of

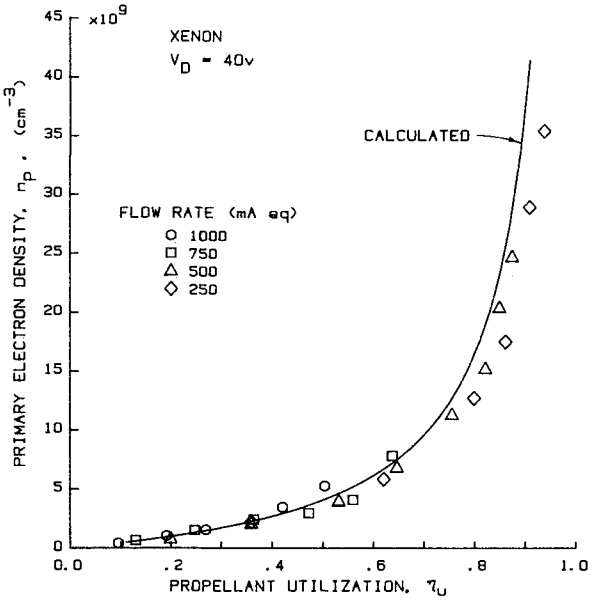

Fig. 3 Primary electron density variation for xenon.

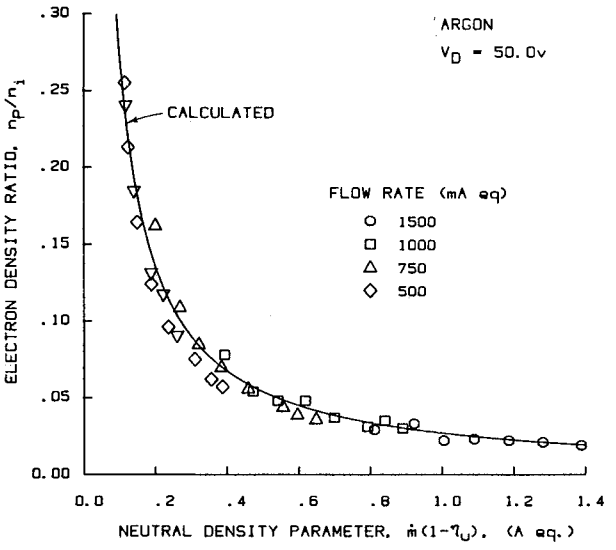

Fig. 4 Primary-to-total electron density ratio variation for argon.

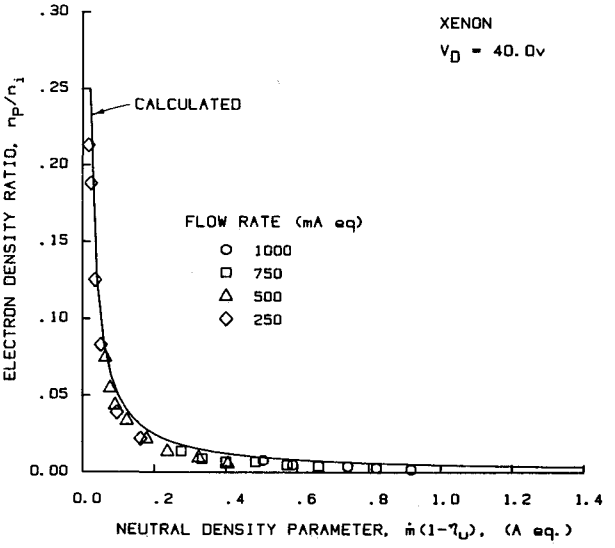

Fig. 5 Primary-to-total electron density ratio variation for xenon.

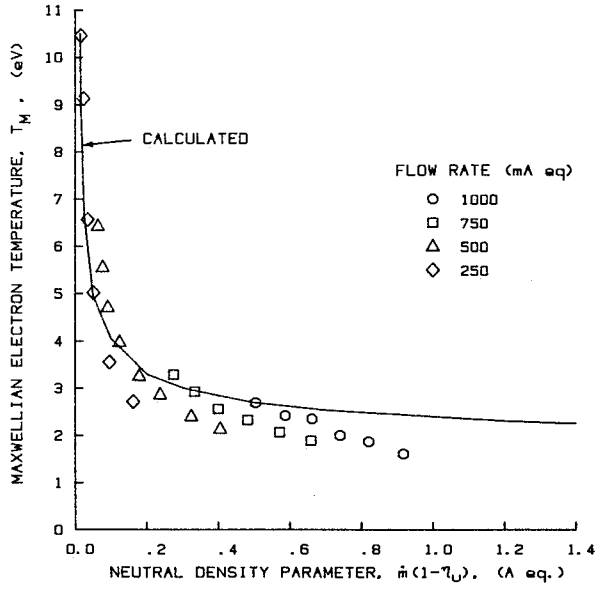

Fig. 6 Maxwellian electron temperature variation for xenon.

the same thruster configuration, but with xenon propellant and a discharge voltage of 40 V. Again, the same conclusions drawn from Fig. 2 are also applicable to thruster operation on xenon as indicated in Fig. 3. The observation that the calculated average values are somewhat greater than the measured centerline values probably results from the use of the measured value of $\epsilon_p^* = 44$ eV in Eq. (21) rather than the calculated value of $\epsilon_p^* = 36$ eV given in the Appendix.

An expression for the ratio of primary-to-total electron density is given by Eq. (24). The combination of parameters in the square brackets in this equation is approximately a constant for a given propellant, discharge voltage and thruster configuration. For operation with argon at $V_D = 50$, Eq. (24) becomes

$$\frac{n_p}{n_i} = \frac{0.027}{\dot{m}(1-\eta_u)} \tag{34}$$

In making this calculation, the Bohm velocity v_b was calculated based on an electron temperature of 4 eV. The value of the screen grid transparency to ions ϕ_i was determined experimentally by measuring the ion current to the screen grid and to the beam. The transparency is then the ratio of the beam current to the sum of the screen grid and beam currents. The measured screen grid transparency to ions was approximately 0.8 compared to the physical open area fraction of the screen grid, which was approximately 0.68.

Comparison of Eq. (34) with the experimentally measured values is given in Fig. 4. This figure indicates that for a given discharge voltage, propellant and thruster configuration the primary-to-total electron density ratio is only a function of the neutral density parameter. In addition, it indicates that Eq. (34) has the correct functional form for the variation of this ratio with the neutral density parameter.

For operation of the same thruster configuration with xenon at $V_D = 40$ V, the results shown in Fig. 5 were obtained. The solid line in this figure corresponds to Eq. (24), where the constant was calculated using values of the parameters in Eq. (24) that are appropriate for xenon propellant and a discharge voltage of 40 V. Figures 4 and 5 indicate that Eq. (24) correctly accounts for changes in the propellant gas, discharge voltage, neutral density parameter, and propellant flow rate.

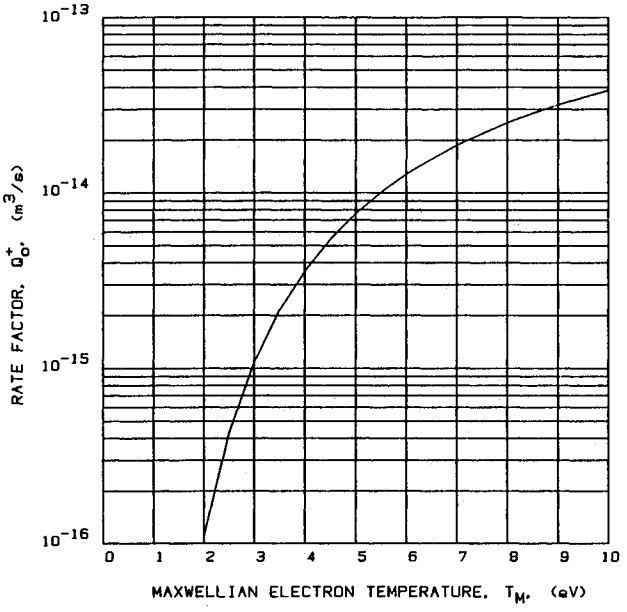

Fig. 7 Ionization rate factor for xenon.

Maxwellian Electron Temperature

Comparison of calculated and measured Maxwellian electron temperatures is given in Fig. 6. The calculated electron temperatures were obtained using Eq. (30). For operation with xenon at $V_D = 40$ V, Eq. (30) becomes

$$Q_0^+ = \frac{7.64 \times 10^{-14}}{226\dot{m}(1-\eta_u) - 1}, \text{ m}^3/\text{s} \tag{35}$$

where the appropriate cross section data were obtained from Refs. 5 and 6. Equation (35) gives the value of the Maxwellian ionization rate factor for the production of single ions from neutral atoms as a function of the neutral density parameter. The rate factor Q_0^+ is a function of the Maxwellian electron temperature T_M and is given by

$$Q_0^+ = \frac{\sqrt{2e/m_e}\int_0^\infty \sigma_+(E)\,E e^{-E/T_M}\,\mathrm{d}E}{\int_0^\infty E^{1/2} e^{-E/T_M}\,\mathrm{d}E} \tag{36}$$

Using Eq. (36), the rate factor Q_0^+ may be plotted as a function of the electron temperature as shown in Fig. 7.

To determine the electron temperature as a function of the neutral density parameter, the following procedure is used. First, the value of the rate factor Q_0^+ is calculated for a given value of $\dot{m}(1-\eta_u)$ using Eq. (35). This value of Q_0^+ is then used to enter the curve in Fig. 7 from which the corresponding electron temperature is determined. Repeating this procedure generates the curve of Maxwellian electron temperature vs neutral density parameter shown as the solid line in Fig. 6. The agreement between the calculated and measured electron temperatures is considered to be quite good.

Conclusions

Simple algebraic equations have been developed to calculate the average values of several discharge chamber plasma properties as functions of the ion source operating conditions. These properties include: the primary electron density, the primary-to-total and primary-to-Maxwellian electron density ratios, and the Maxwellian electron temperature. The primary electron density is a strong function of the propellant utilization efficiency, but is independent of the propellant flow rate into the discharge chamber and the primary electron containment length. The primary-to-total and primary-to-Maxwellian density ratios and the Maxwellian electron temperature are influenced most strongly by the neutral density parameter $\dot{m}(1-\eta_u)$. Each of the plasma properties calculated by the model agrees well with the corresponding experimental data for both argon and xenon gases.

Appendix: Theoretical Calculation of the Baseline Plasma Ion Energy Cost ϵ_p^*

A simple technique for the calculation of the baseline plasma ion energy cost has also been developed and is given in this Appendix. Calculations using this technique are shown to agree well with previously measured values of ϵ_p^*. The definition of the baseline plasma ion energy cost ϵ_p^* is given by[7]

$$\epsilon_p^* = \frac{\epsilon_0 + \epsilon_M}{1 - (V_C + \epsilon_M)/V_D} \tag{A1}$$

where V_C is the plasma potential from which electrons emitted by the cathode are accelerated to become primary electrons (for thermionic cathodes $V_C = 0$). The parameter ϵ_0 in Eq. (A1) accounts for the energy that is expended in ionization and excitation reactions and is defined by

$$\epsilon_0 \equiv U_+ + \frac{\Sigma_j \langle \sigma_j v_e \rangle U_j}{\langle \sigma_+ v_e \rangle} \tag{A2}$$

where U_+ is the ionization energy, U_j the excitation energy of the jth excited atomic state, and the summation is over the set of excited atomic states. The brackets in this equation represent the enclosed product averaged over the entire electron speed distribution function, i.e.,

$$\langle \sigma_+ v_e \rangle = \frac{\int_0^\infty \sigma_+(v_e)\, v_e F(v_e)\,\mathrm{d}v_e}{\int_0^\infty F(v_e)\,\mathrm{d}v_e} \tag{A3}$$

where $F(v_e)$ represents the entire electron distribution function.

For a plasma with an electron population characterized by a Maxwellian distribution of temperature T_M and a monoenergetic (primary) group of energy E_p, Eq. (A2) becomes

$$\epsilon_0 = U_+ + \frac{\Sigma_j \left[(n_p/n_M)\,\sigma_j' v_p + \langle \sigma_j v_e \rangle_M \right] U_j}{(n_p/n_M)\,\sigma_+' v_p + \langle \sigma_+ v_e \rangle_M} \tag{A4}$$

where $\langle\ \rangle_M$ represents the enclosed product averaged over the Maxwellian speed distribution function.

The term under the summation sign in Eq. (A4) may be approximated by considering only a single equivalent lumped excited state characterized by a total excitation collision cross section σ_{ex} and a lumped excitation energy U_{ex}. For rare gases, U_{ex} may be approximated by[8]

$$U_{ex} = \tfrac{1}{2}(U_l + U_+) \tag{A5}$$

where U_l is the lowest excitation energy level. Using this lumped excitation approximation and combining Eqs. (A1) and (A4) yields the following expression for ϵ_p^*,

$$\epsilon_p^* = \frac{U_+ + \epsilon_M + \dfrac{\left[\dfrac{n_p}{n_M}\sigma_{ex}' v_p + \langle \sigma_{ex} v_e \rangle_M\right] U_{ex}}{\dfrac{n_p}{n_M}\sigma_+' v_p + \langle \sigma_+ v_e \rangle_M}}{1 - \dfrac{(V_C + \epsilon_M)}{V_D}} \tag{A6}$$

The value of ϵ_p^* may be easily calculated using Eq. (A6) for a given Maxwellian electron temperature, primary-to-Maxwellian electron density ratio, discharge voltage, and value of V_C. In addition, the average energy of a Maxwellian electron lost

to the anode ϵ_M must be known. Reference 9 gives this energy as

$$\epsilon_M = 2T_A + V_A \tag{A7}$$

where T_A is the electron temperature at the anode and V_A the difference between plasma potential and anode potential. Experiments were performed to determine the relationship between the electron temperature at the anode and the bulk plasma electron temperature. These experiments used two Langmuir probe assemblies, one positioned on the thruster centerline and the other on the upstream magnet ring. This second probe was used to measure the temperature of the Maxwellian electrons and the energy of the primary electrons reaching the anode. Because the probe was positioned in a region of very high magnetic flux density, the electron temperatures determined from the traces obtained with this probe are probably only equal to the electron temperature resulting from motion along the magnetic field lines. The electron temperature corresponding to motion normal to the field lines may or may not be the same. Nevertheless, for simplicity, these temperatures are assumed here to be the same.

The measured electron temperatures at the anode were found to be about two-thirds of the measured centerline temperatures. The correlation of electron temperature at the anode with the centerline electron temperature is given in Fig. A1. The data in this figure were obtained using both argon and xenon propellants. The solid line in this figure has a 2/3 slope. This observation that the electron temperature at the anode is approximately two-thirds of the centerline temperature may be used to calculate the baseline plasma ion energy cost ϵ_p^*. Therefore, ϵ_M will be taken as

$$\epsilon_M = 2\left(\frac{2}{3}T_M\right) + V_A \tag{A8}$$

Langmuir probe measurements also indicate that for the thruster configurations tested in this investigation V_A was always approximately 2 V; thus, this value of V_A will be used in Eq. (A8) for these calculations.

For xenon, the values of the total excitation collisions cross section required by Eq. (A6) were taken from Ref. 6. Ionization cross-sectional data were obtained from Ref. 7. With these data, Eq. (A6) was used to calculate the values of ϵ_p^* as a function of electron temperature with the primary-to-Maxwellian electron density ratio as a parameter. The results of these calculations are given in Fig. A2 where the values $V_D = 40$ V, $V_C = 0$ V, and $V_A = 2$ V were used. From this figure, it is seen that the baseline plasma ion energy cost can vary over a wide range of values; it is not clear at this point which value or values of ϵ_p^* are appropriate. This difficulty arises because the Maxwellian electron temperature and primary-to-Maxwellian electron density ratio may not be selected independently as was done for the calculations in Fig. A2.

To resolve this difficulty, a second equation for ϵ_p^* is required. This second equation may be derived in the following manner. Equation (12) provides an expression for the ratio of ion current produced by primary electrons to the total ion current produced, i.e.,

$$\frac{J_p'}{J_p} = \frac{\epsilon_p^* \sigma_+'}{V_D \sigma_0'} \tag{A9}$$

The total ion current produced, however, is given by

$$J_p = n_0 n_p e v_p \sigma_+' \forall + n_0 n_M e \langle \sigma_+ v_e \rangle_M \forall \tag{A10}$$

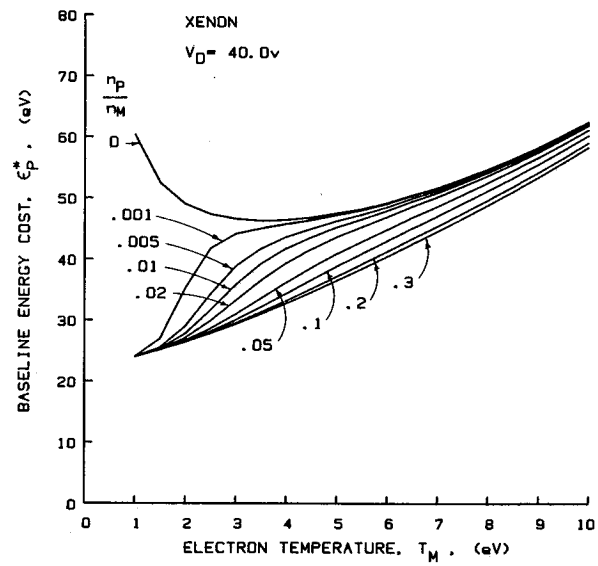

Fig. A2 Baseline plasma ion energy cost variation calculated from Eq. (A6) for xenon.

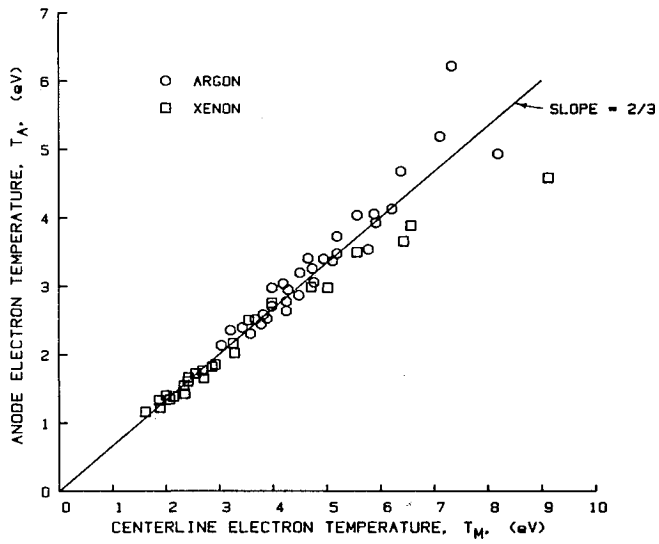

Fig. A1 Correlation of electron temperatures.

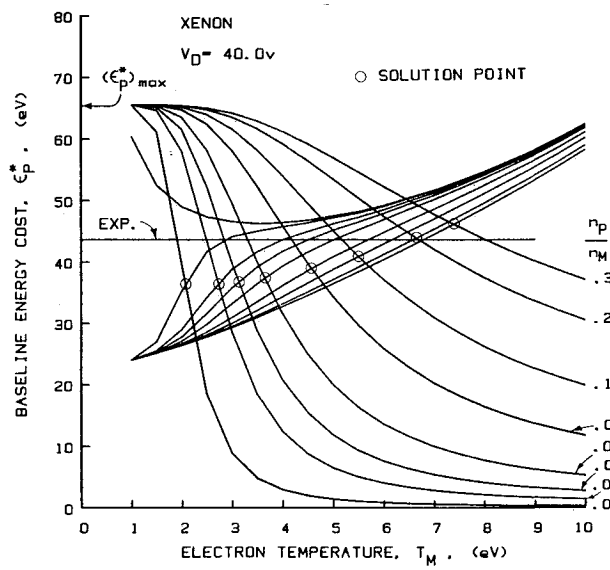

Fig. A3 Solutions for the baseline plasma ion energy cost for xenon.

and the ion current produced by primary electrons is given by Eq. (2) as

$$J_p' = n_0 n_p e v_p \sigma_+' V \tag{A11}$$

dividing Eq. (A11) by Eq. (A10) yields

$$\frac{J_p'}{J_p} = \frac{1}{1 + \left(n_M \langle \sigma_+ v_e \rangle_M / n_{p'_+} v_p \right)} \tag{A12}$$

Equating Eq. (A12) to Eq. (A9) and solving for ϵ_p^* yields the desired second equation for the baseline plasma ion energy cost,

$$\epsilon_p^* = \frac{V_D \sigma_0' / \sigma_+'}{1 + \left(n_M \langle \sigma_+ v_e \rangle_M / n_p \sigma_+' v_p \right)} \tag{A13}$$

The appropriate values of ϵ_p^*, determined from the correct corresponding electron temperatures and density ratios, may be found by solving Eqs. (A6) and (A13) simultaneously for ϵ_p^* and the electron temperature for specified values of the primary-to-Maxwellian electron density ratio. This procedure is most easily accomplished graphically, as shown in Fig. A3, where the intersection of the curves corresponding to the same values of n_p/n_M gives both ϵ_p^* and the electron temperature. The locus of these intersection points indicates the variation of the baseline plasma ion energy cost with the electron temperature and primary-to-Maxwellian electron density ratio. Figure A3 indicates that, under the assumptions used for these calculations, ϵ_p^* does not vary substantially over wide variations in electron temperature and n_p/n_M. This agrees with the experimental observation[7] that ϵ_p^* is a constant for operation with xenon propellant at a discharge voltage of 40 V.

The measured value of ϵ_p^* from Ref. 7 is shown along with the calculated values in Fig. A3. At low electron temperatures, the experimental value is seen to be generally slightly higher than the calculated values. The most likely explanation for this is a systematic measurement error of the total ion current produced due to the inability to measure the ion current to the anode potential surfaces. Also indicated in Fig. A3 is the theoretical maximum value of ϵ_p^* for this case [as calculated from Eq. (13)]. Finally, it should be noted that the above results are somewhat sensitive to the choice of ϵ_M, which is assumed here to be given by Eq. (A8).

References

[1] Brophy, J.R. and Wilbur, P.J., "Simple Performance Model for Ring and Line Cusp Ion Thrusters," *AIAA Journal*, Vol. 23, Nov. 1985, pp. 1731-1736.

[2] Bohm, D., "Minimum Ionic Kinetic Energy for a Stable Sheath," *Characteristics of Electrical Discharges in Magnetic Fields*, edited by A. Guthrie and R.K. Wakerling, McGraw-Hill Book Co., New York., 1949.

[3] Brophy, J.R. and Wilbur, P.J., "An Experimental Investigation of Cusped Magnetic Field Discharge Chambers," *AIAA Journal*, Vol. 24, Jan. 1986, pp. 21-26.

[4] Clausing P., "Uber Die Stromung Sehr Verdunnter Case Durch Roren Von Beliebiger Lange," *Annalen Der Physik*, Vol. 12, 1932, pp. 961-989.

[5] Rapp, D. and Englander-Golden, P., "Total Cross Sections for Ionization and Attachment in Gases by Electron Impact: I. Positive Ionization," *Journal of Chemical Physics*, Vol. 34, No. 5, 1965, pp. 1464-1479.

[6] Hayashi, M., "Determination of Electron-Xenon Total Excitation Cross Sections, from Threshold to 100 eV, from Experimental Values of Townsend's α," *Journal of Physics D: Applied Physics*, Vol. 16, 1983, pp. 581-589.

[7] Brophy, J.R., "Ion Thruster Performance Model," NASA CR-174810, Dec. 1984.

[8] Dugan, J.V. and Sovie, R.J., "Volume Ion Production Costs in Tenuous Plasmas: A General Atom Theory and Detailed Results for Helium, Argon and Cesium," NASA TN D-4150, 1967.

[9] Divergilio, W.F., Goede, H., and Fosnight, V.V., "High Frequency Plasma Generators for Ion Thrusters," Interim Report, NASA CR-167957, 1981.